
Instance Selection for GANs

Terrance DeVries
 University of Guelph
 Vector Institute

Michal Drozdzal
 Facebook AI Research

Graham W. Taylor
 University of Guelph
 Vector Institute
 Canada CIFAR AI Chair

Abstract

Recent advances in Generative Adversarial Networks (GANs) have led to their widespread adoption for the purposes of generating high quality synthetic imagery. While capable of generating photo-realistic images, these models often produce unrealistic samples which fall outside of the data manifold. Several recently proposed techniques attempt to avoid spurious samples, either by rejecting them after generation, or by truncating the model’s latent space. While effective, these methods are inefficient, as large portions of model capacity are dedicated towards representing samples that will ultimately go unused. In this work we propose a novel approach to improve sample quality: altering the training dataset via instance selection before model training has taken place. To this end, we embed data points into a perceptual feature space and use a simple density model to remove low density regions from the data manifold. By refining the empirical data distribution before training we redirect model capacity towards high-density regions, which ultimately improves sample fidelity. We evaluate our method by training a Self-Attention GAN on ImageNet at 64×64 resolution, where we outperform the current state-of-the-art models on this task while using $1/2$ of the parameters. We also highlight training time savings by training a BigGAN on ImageNet at 128×128 resolution, achieving a 66% increase in Inception Score and a 16% improvement in FID over the baseline model with less than $1/4$ the training time.

1 Introduction

Recent advances in Generative Adversarial Networks (GANs) have enabled these models to be considered a tool of choice for vision synthesis tasks that demand high fidelity outputs, such as image and video generation [5, 11], image editing [36], inpainting [30], and superresolution [27]. However, when sampling from a trained GAN model, the image quality is oftentimes uneven, and outputs may be unrealistic just as often as they appear photo-realistic.

GANs fit a model to a data distribution with the help of a discriminator network. Low quality samples produced by these models are often attributed to poor modeling of the low-density regions of the data manifold [10]. The majority of current techniques attempt to eliminate low quality samples after the model is trained, either by changing the model distribution by truncating the latent space [2, 10] or by performing some form of rejection sampling using a trained discriminator to inform the rejection process [1, 4, 26]. Nevertheless, these methods are inefficient with respect to model capacity and training time, since much of the capacity and optimization efforts dedicated to representing the sparse regions of the data manifold is wasted.

In this paper, we analyze the use of instance selection [20] in the generative setting. We address the problem of uneven model sample quality before GAN model training has begun, rather than after it has finished. We note that dataset collection is a noisy process, and that most of the currently used datasets for generative model training and evaluation were not purposely created for this task. Thus, through a dataset curation step, we remove low density regions from the data manifold prior to model optimization and show that this *direct* dataset intervention (1) reduces the probability of low

quality image samples, (2) reduces model capacity and training time requirements, and (3) can be combined with existing sample filtering techniques to further improve generation quality. To remove the sparsest parts of the image manifold we first project the images into an embedding space of perceptually meaningful representations. Next, we fit a scoring function to assess the manifold density in the neighbourhood of each embedded data point in the dataset. In the final step, we remove the data points from the dataset with the lowest manifold density score. In our experiments, we evaluate a variety of image embeddings and scoring functions, observing that Inceptionv3 and Gaussian likelihood are well suited for the respective roles. Overall, we make the following contributions:

- We propose dataset curation via instance selection to improve the output quality of GANs.
- We show that the manifold density in the perceptual embedding space of a given dataset is predictive of GAN performance, and therefore a good scoring function for instance selection.
- We demonstrate the *model capacity savings* of instance selection by achieving state-of-the-art performance on 64×64 resolution ImageNet generation using a Self-Attention GAN with $1/2$ the amount of trainable parameters of the current best model.
- We demonstrate *training time savings* by training a 128×128 resolution BigGAN on ImageNet in $1/4$ the time of the baseline, while also improving Inception Score by 66% and Fréchet Inception Distance (FID) by 16% (computed w.r.t. the *unaltered data distribution*).

2 Related Work

Generative modelling of images is a very challenging problem due to the high dimensional nature of images and the complexity of the distributions they form. Several different approaches towards image generation have been proposed, with GANs currently being state-of-the-art in terms of image generation quality. In this work we will focus primarily on GANs, but other types of generative models might also benefit from instance selection prior to model fitting.

2.1 Sample Filtering in GANs

One way to improve the sample quality from GANs without making any changes to the architecture or optimization algorithm is by applying techniques which automatically filter out poor quality samples from a trained model. Discriminator Rejection Sampling (DRS) [1] accomplishes this by performing rejection sampling on the generator. This process is informed by the discriminator, which is reused to estimate density ratios between the real and generated image manifolds. Metropolis-Hastings GAN (MH-GAN) [26] builds on DRS by i) calibrating the discriminator to achieve more accurate density ratio estimates, and by ii) applying Markov chain Monte Carlo (MCMC) instead of rejection sampling for better performance on high dimensional data. Ding et al. [7] further improve density ratio estimates by fine-tuning a pretrained ImageNet classifier for the task. For more efficient sampling, Discriminator Driven Latent Sampling (DDLS) [4] iteratively updates samples in the latent space to push them closer to realistic outputs.

Instead of filtering samples after the GAN has been trained, some methods do so during the training procedure. Latent Optimisation for Generative Adversarial Networks (LOGAN) [28] optimizes latent samples each iteration at the cost of an additional forward and backward pass. Sinha et al. [23] demonstrate that gradients from low quality generated samples drive the model away from the nearest mode rather than towards it. As such, gradients from the worst samples each iteration during training may be ignored to improve generation quality.

Perhaps the most well known approach for increasing sample fidelity in GANs is the “truncation trick” [2, 10, 15]. The truncation trick is used in the popular models BigGAN [2] and StyleGAN [10, 11] to improve image quality by manipulating the latent distribution. The original truncation trick as used by BigGAN consists of replacing the latent distribution with a truncated distribution during inference, such that any latent sample that falls outside of some acceptable range is resampled. StyleGAN uses a similar strategy by interpolating samples towards the mean of the latent space instead of resampling them. By moving samples closer to the interior regions of the latent space, sample diversity can effectively be traded for visual fidelity.

2.2 Instance Selection

Instance selection is a data preprocessing technique commonly used in the classification setting to select a subset of data from a larger collection [20]. In general, there are two main approaches to instance selection: wrapper methods, and filter methods. Wrapper methods attempt to reduce the size of the dataset to a more manageable size while preserving samples along class boundaries, while filter methods try to clean the dataset by eliminating noisy samples near class boundaries. Though commonly used in the setting of big data, instance selection has received little attention from the generative modelling community. Nuha et al. [19] explore the impact of reducing the size of the training set when training GANs. However, they select data points randomly, and no significant improvement in performance is observed from the removal of data.

3 Instance Selection for GANs

In the context of generative modeling, our motivation is to automatically remove the sparsest regions of the data manifold, specifically those parts that GANs struggle to capture. To do so, we define an image embedding function F and a scoring function H .

Embedding function F projects images into an embedding space. More precisely, given a dataset of images \mathcal{X} , the dataset of embedded images \mathcal{Z} is obtained by applying the embedding function $\mathbf{z} = F(\mathbf{x})$ to each data point $\mathbf{x} \in \mathcal{X}$. For the task of image generation we suggest using perceptually aligned embedding functions [32], such as the feature space of a pretrained image classifier.

Scoring function H is used to to assess the manifold density in a neighbourhood around each embedded data point \mathbf{z} . In our experiments, we compare three choices of scoring function: log likelihood under a standard Gaussian model, log likelihood under a Probabilistic Principal Component Analysis (PPCA) [25] model, and distance to the K^{th} nearest neighbour (KNN Distance). We select Gaussian and PPCA as simple, well known density models. KNN Distance has previously been used as a measure of local manifold density in classical instance selection [3], and has been shown to be useful for defining non-linear image manifolds [13, 18].

The Gaussian model is fit to the embedded dataset by computing the empirical mean $\boldsymbol{\mu}$ and the sample covariance $\boldsymbol{\Sigma}$ of \mathcal{Z} . The score of each embedded image \mathbf{z} is computed as follows:

$$H_{\text{Gaussian}}(\mathbf{z}) = -\frac{1}{2}[\ln(|\boldsymbol{\Sigma}|) + (\mathbf{z} - \boldsymbol{\mu})^T \boldsymbol{\Sigma}^{-1}(\mathbf{z} - \boldsymbol{\mu}) + d \ln(2\pi)], \quad (1)$$

where d is the dimension of \mathbf{z} .

PPCA is fit to the embedded dataset using any standard PPCA solver [21]. We set the number of principal components such that 95% of the variance in the data is preserved. Embedded images are scored as follows:

$$H_{\text{PPCA}}(\mathbf{z}) = -\frac{1}{2}[\ln(|\mathbf{C}|) + \text{Tr}((\mathbf{z} - \boldsymbol{\mu})^T \mathbf{C}^{-1}(\mathbf{z} - \boldsymbol{\mu})) + d \ln(2\pi)], \quad \mathbf{C} = \mathbf{W}\mathbf{W}^T + \sigma^2\mathbf{I}, \quad (2)$$

where \mathbf{W} is the fit model weight matrix, $\boldsymbol{\mu}$ is the empirical mean of \mathcal{Z} , σ is the residual variance, \mathbf{I} is the identity matrix, and d is the dimension of \mathbf{z} .

KNN Distance is used to score data points by calculating the Euclidean distance between \mathbf{z} and $\mathcal{Z} \setminus \{\mathbf{z}\}$, then returning the distance to the K^{th} nearest element. We make the resulting distance negative, such that smaller distances return larger values. Formally, we can evaluate:

$$H_{\text{KNN}}(\mathbf{z}, K, \mathcal{Z}) = -\min_K \left\{ \|\mathbf{z} - \mathbf{z}_i\|_2 \quad : \quad \mathbf{z}_i \in \mathcal{Z} \setminus \{\mathbf{z}\} \right\}, \quad (3)$$

where \min_K is defined as the K^{th} smallest value in a set. In our experiments we set $K = 5$.

To perform **instance selection**, we compute scores $H(F(\mathbf{x}))$ for each data point and keep all data points with scores above some threshold ψ . For convenience, we often set ψ to be equal to some percentile of the scores, such that we preserve the top $N\%$ of the best scoring data points. Thus, given an initial training set consisting of data points $\mathbf{x} \in \mathcal{X}$ we construct our reduced training set \mathcal{X}' by computing:

$$\mathcal{X}' = \{\mathbf{x} \in \mathcal{X} \quad \text{s.t.} \quad H(F(\mathbf{x})) > \psi\}. \quad (4)$$



(a) Images with highest likelihood



(b) Images with least likelihood

Figure 1: Examples of the (a) most and (b) least likely resized images of red foxes from the ImageNet dataset, as determined by a Gaussian model fit on images in an Inceptionv3 embedding space. High likelihood images share a similar visual structure, while low likelihood samples are more varied.

To illustrate why removing data points from the training set might be a good idea, we look at the most and least likely images from the red fox class of ImageNet (Figure 1). Likelihood is determined by a Gaussian model fit on feature embeddings from a pretrained Inceptionv3 classifier. We notice a stark contrast between the content of the images. The most likely images (a) are similarly cropped around the fox’s face, while the least likely images (b) have many odd viewpoints and often suffer from occlusion. It is logical to imagine how a generative model trained on these unusual instances may try to generate samples that mimic such conditions, resulting in nonsensical outputs.

4 Experiments

In this section we review evaluation metrics, motivate selecting instances based on manifold density, and then analyze the impact of applying instance selection to GAN training.

4.1 Evaluation Metrics

We use a variety of evaluation metrics to diagnose the effect that training with instance selection has on the learned distribution, including: (1) Inception Score (IS) [22], (2) Fréchet Inception Distance (FID) [9], (3) Precision and Recall (P&R) [13], and (4) Density and Coverage (D&C) [18]. In all cases where a reference distribution is required we use *the original training distribution*. Using the distribution produced after instance selection would unfairly favour the evaluation of instance selection, since the reference distribution could be changed to one that is trivially easy to generate. A detailed description of each evaluation metric is provided in the supplementary material.

When calculating FID we follow Brock et al. [2] in using all images in the training set to estimate the reference distribution, and sampling 50k images to make up the generated distribution. For P&R and D&C we use an Inceptionv3 embedding.¹ N and M are set to 10k samples for both the reference and generated distributions, and K is set equal to 5 as recommended by Naeem et al. [18].

4.2 Relationship Between Dataset Manifold Density and GAN Performance

An image manifold is more accurately defined in regions where many data points are in close proximity to each other [13]. Since GANs attempt to reproduce an image manifold based on data points from a given dataset, we suspect that they should perform better on datasets with well-defined manifolds (i.e. no sparse manifold regions). To verify this hypothesis, we use the ImageNet² dataset [6] and treat each of the 1000 classes as a separate dataset. Ideally, we would fit a separate GAN on each class to obtain a ground truth measure of performance, but this is very computationally expensive. Instead, we use a single class-conditional BigGAN from [2] that has been pretrained on ImageNet at 128×128 resolution. For each class, we sample 700 real images from the dataset, and generate 700 class-conditioned samples with the BigGAN. To measure the density for each class manifold we compare three different methods: Gaussian likelihood, Probabilistic Principal Component Analysis (PPCA) likelihood, and distance to the K^{th} neighbour (KNN Distance) (§3). Images are projected into the feature space of an Inceptionv3 model, and a manifold density score is computed on the

¹We use the PyTorch pretrained Inceptionv3 model. As this model yields slightly different results than the official TensorFlow Inceptionv3 model, we only compare to other models that use the PyTorch implementation.

²Use of ImageNet is only for noncommercial, research purposes, and not for training networks deployed in production or for other commercial uses.

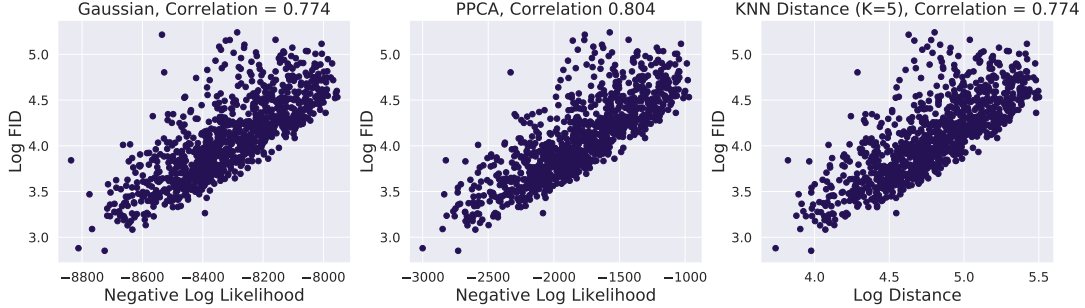


Figure 2: Correlation between manifold density estimates and FID for each class in the ImageNet dataset. Lower values on the x-axis indicate a more dense dataset manifold. Lower values on the y-axis indicate better quality generated samples.

features using one of our scoring functions. As an indicator of the true GAN output quality we compute FID between the real and generated distributions for each class.

We observe a strong correlation between each of the manifold density measures and GAN output quality (Figure 2). This correlation confirms our hypothesis, suggesting that dataset manifold density is an important factor for achieving high quality generated samples with GANs.

4.3 Embedding and Scoring Function

Having established that dataset manifold density is correlated with GAN performance, we explore artificially increasing the overall density of the training set by removing data points that lie in low density regions of the data manifold. To this end, we train several Self-Attention GANs (SAGAN) [31] on ImageNet at 64×64 resolution. Each model is trained on a different 50% subset of ImageNet, as chosen by instance selection using different embedding and scoring functions as described in §3. We use the default settings for SAGAN, except that we use a batch size of 128 instead of 256, apply the self-attention module at 32×32 resolution instead of 64×64 , and reduce the number of channels in each layer by half in order to reduce the computational cost of our initial exploratory experiments. All models are trained for 200k iterations. The results of these experiments are shown in Table 1.

All runs utilizing instance selection significantly outperform the baseline model trained on the full dataset, despite only having access to half as much training data. Inception Score increases by as much as 66% and FID decreases by up to 41% (Table 1). While a high Inception Score could be achieved by the GAN overfitting on a single image per class, the decrease in FID confirms that this is not the case. To verify that the gains are not simply caused by the reduction in dataset size we train a model on a 50% subset that was uniform-randomly sampled from the full dataset. Here, we observe little change in performance compared to the baseline, indicating that performance improvements are indeed due to careful selection of training data, rather than reducing the size of the dataset.

Table 1: Comparison of embedding and scoring functions. Models trained with instance selection significantly outperform models trained without instance selection, despite training on a fraction of the available data. RR is the retention ratio (percentage of dataset trained on). Best results in bold.

Instance Selection	RR (%)	Embedding	Pretraining Dataset	IS \uparrow	FID \downarrow	P \uparrow	R \uparrow	D \uparrow	C \uparrow
None	100	-	-	15.41	21.35	0.66	0.62	0.64	0.64
Uniform	50	-	-	15.46	22.78	0.65	0.62	0.65	0.65
Gaussian	50	Inceptionv3	ImageNet	25.68	12.57	0.77	0.59	0.97	0.83
PPCA	50	Inceptionv3	ImageNet	25.52	13.17	0.76	0.58	0.97	0.82
KNN Dist	50	Inceptionv3	ImageNet	25.42	13.05	0.76	0.58	0.97	0.82
Gaussian	50	Inceptionv3	Random init	15.47	21.91	0.66	0.61	0.68	0.65
Gaussian	50	ResNet-50	Places365	20.64	16.52	0.74	0.59	0.88	0.76
Gaussian	50	ResNeXt-101	Instagram 1B	24.11	14.10	0.73	0.61	0.86	0.80

We find that all three candidate scoring functions, Gaussian likelihood, PPCA likelihood, and KNN distance, significantly outperform the full dataset baseline. Gaussian likelihood scores slightly better than the alternatives, so we use it as the scoring function in the remainder of our experiments.

To understand the importance of the embedding function, we compare several different model embeddings that have been trained on different datasets: Inceptionv3 [24] trained on ImageNet, ResNet50 [8] trained on Places365 [35], and ResNeXt-101 32x8d [29] trained with weak supervision on Instagram 1B [14]. We also compare a randomly initialized Inceptionv3 with no pretraining as a random embedding. Inceptionv3, ResNet-50, and ResNeXt-101 features are all extracted after the global average pooling layer. We find that all feature embeddings improve performance over the full dataset baseline except for the randomly initialized network. These results suggest that an embedding function that is well aligned with the target domain is required in order for instance selection to be effective. The ImageNet pretrained Inceptionv3 embedding performs best overall, and was chosen as the embedding function for the rest of our experiments.

4.4 Retention Ratio

An important consideration when performing instance selection is determining what proportion of the original dataset to keep. To investigate the impact of the retention ratio hyperparameter on training, we train ten SAGANs on ImageNet, each retaining different amounts of the original dataset in 10% intervals. GAN hyperparameters are the same as in §4.3, except that we extend training until 500k iterations in order to observe model behaviours over a longer training window.

Performance on almost all metrics (Inception Score, FID, Precision, Density, and Coverage) consistently improves as larger portions of the original dataset are removed (Figure 3, Table 3). However, removing too much of the dataset leads some models to collapse prematurely, before they have fully trained. As such, finding the right balance between performance and volatility is crucial as removing too many or too few data points will result in sub-optimal performance. As a rule of thumb when applying instance selection to GANs, we suggest to first reduce a dataset by 50%, and then incrementally reduce the retention ratio until the model experiences early collapse.

Our best performing SAGAN model in terms of FID was trained on only 40% of the ImageNet dataset, yet *outperforms* FQ-BigGAN [34], the current state-of-the-art model for the task of 64×64 ImageNet generation. Despite using $2 \times$ less parameters and a $4 \times$ smaller batch size, our SAGAN achieves a better Inception Score (37.09 vs. 29.96) and FID (9.07 vs. 9.76). As indicated by these scores and the errors made by a pretrained classifier, samples from our instance selection model are significantly more recognizable than those from the baseline model trained on the full dataset (Figure 4).

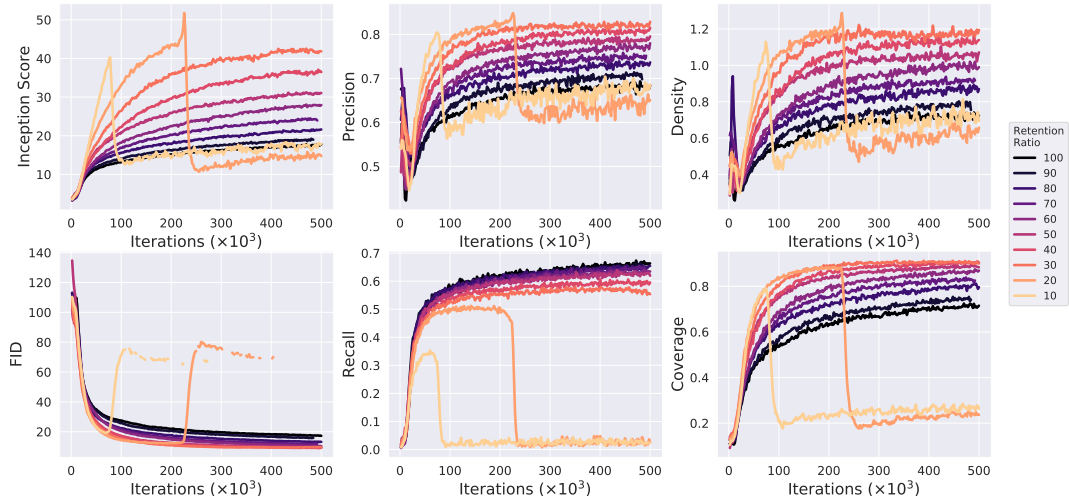
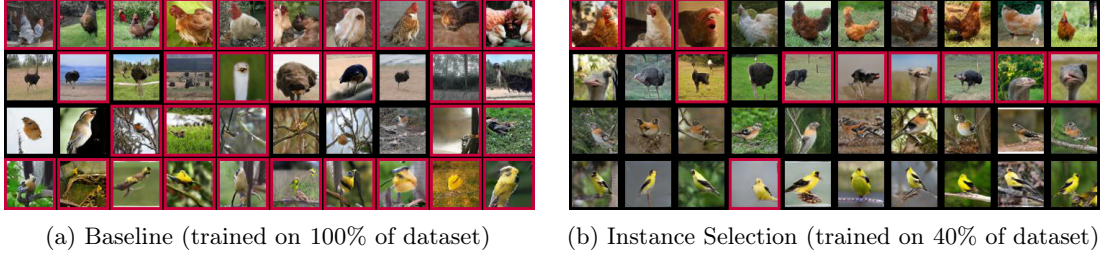


Figure 3: SAGAN trained on 64×64 ImageNet, with instance selection used to reduced the dataset by varying amounts. Retention ratio = 100 indicates a model trained on the full dataset (i.e. no instance selection). The application of instance selection boosts performance significantly.



(a) Baseline (trained on 100% of dataset)

(b) Instance Selection (trained on 40% of dataset)

Figure 4: Samples of bird classes from SAGAN trained on 64×64 ImageNet. Each row is conditioned on a different class. Red borders indicate misclassification by a row-specific pretrained Inceptionv3 classifier. Instance selection (b) significantly improves sample fidelity compared to the baseline (a).

4.5 Complementarity of Instance Selection and Truncation

The truncation trick is a simple and popular technique which is used to increase the visual fidelity of samples from a GAN at the expense of reduced diversity [2]. This trade-off is achieved by biasing latent samples towards the interior regions of the latent distribution, either by truncating the distribution, or by interpolating latent samples towards the mean [10, 13].

To examine the compatibility between the truncation trick and instance selection, we truncate latent vectors of the models trained in §4.4, varying the truncation threshold from 1.0 to 0.1 (Figure 5). We observe that combining both techniques results in a greater improvement in visual fidelity than either method applied in isolation. We anticipate that other post-hoc filtering methods could also see complimentary benefits when combined with instance selection, such as DRS, MH-GAN, and DDLS.

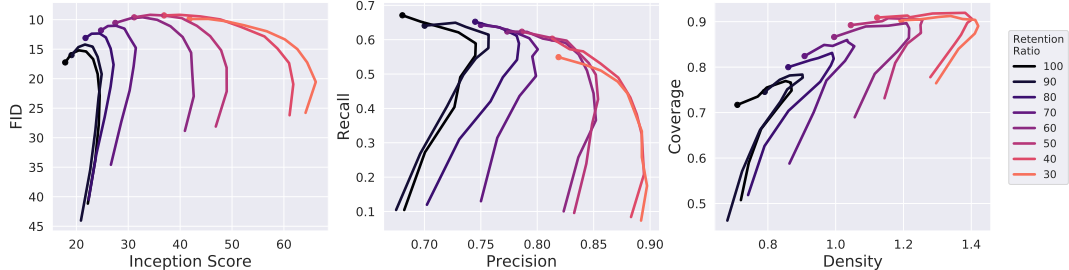


Figure 5: Truncation trick applied to models trained with instance selection for truncation thresholds 1 to 0.1. The base models (threshold = 1) are marked with a \bullet . Up and to the right is best.

4.6 128×128 ImageNet

To examine the impact of instance selection on the training time of large scale models, we train two BigGAN models on 128×128 ImageNet.³ Our baseline model uses the default hyperparameters from BigGAN [2], though we reduce the channel multiplier from 96 to 64 (i.e. half of the capacity) and only use a single discriminator update instead of two for faster training. Our instance selection model uses the same settings as the baseline, but is trained on 50% of the dataset. We also reduce the batch size from the default 2048 to 256 as we encounter worse performance at larger sizes. Both models are trained on 8 V100 GPUs using gradient accumulation to achieve the necessary batch sizes.

Despite using a much smaller batch size, our model trained with instance selection achieves a 66% increase in Inception Score and a 16% decrease in FID over the baseline while training in a quarter of the time (Table 2, Figure 6). Comparing generated samples from both models (Figure 7) we notice that, while the baseline model is still capable of generating high quality samples, it does so much more sporadically than the model trained with instance selection, which is more consistent in its generation quality. We also find that instance selection improves sample quality considerably for classes which have highly varied images in the training set, such as the Mask class. Additional samples can be found in the supplementary material.

³We use the official BigGAN implementation from <https://github.com/ajbrock/BigGAN-PyTorch>.

Table 2: Performance of models on the 128×128 ImageNet image generation task.

Model	Ch	Params (M)	$\text{Itr} \times 10^3$	Batch	$\text{IS} \uparrow$	$\text{FID} \downarrow$	$\text{Time} \downarrow$
BigGAN	64	71.3	186	2048	68.80	11.53	14.75 days
BigGAN + Inst. Sel.	64	71.3	270	256	114.32	9.61	3.66 days

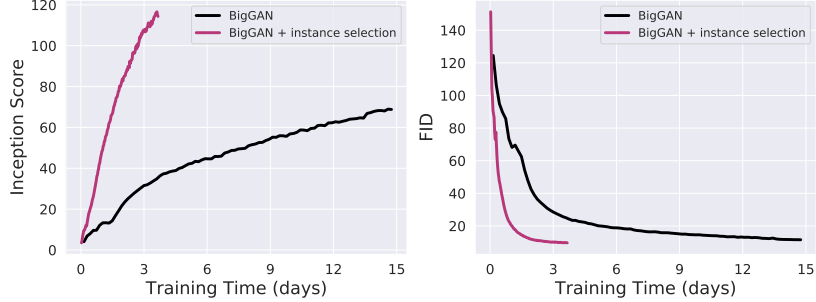


Figure 6: BigGAN models trained on 128×128 ImageNet. The model trained with instance selection converges $4\times$ quicker than the baseline model while achieving better Inception Score and FID.



Figure 7: Representative samples from BigGAN trained on 128×128 ImageNet, without truncation. Each row is conditioned on a different class (from top): EntleBucher, Jack-o’-lantern, and Mask. Models trained without instance selection (a) are much more sporadic with their production of high quality samples than models trained with instance selection (b).

5 Conclusion

Folk wisdom suggests *more data is better*, however, it is known that areas of the data manifold that are sparsely represented pose a challenge to current GANs [10]. To directly address this challenge we introduce a new tool: dataset curation via instance selection. Our motivation is to remove sparse regions of the data manifold before training, acknowledging that they will ultimately be poorly represented by the GAN, and therefore, that attempting to capture them is an inefficient use of model capacity. Moreover, popular post-processing methods such as rejection sampling or latent space truncation will likely ignore these regions as represented by the model. There are several benefits of taking the instance selection approach: (1) We improve sample quality across a variety of metrics compared to training on uncurated data and compared to post-hoc methods; (2) We demonstrate that reallocating model capacity to denser regions of the data manifold leads to efficiency gains: meaning that we can achieve SOTA quality with a smaller-capacity model trained in far less time; and (3) We show that instance selection and truncation are stackable, leading to mutual benefit. To our knowledge, instance selection has not been formally analyzed in the generative setting. However, we argue that it is more important here than in supervised learning because of the absence of an annotation phase where humans often perform some kind of formal or informal curation.

Acknowledgements

The authors would like to thank Colin Brennan, with whom discussions about dataset learnability kicked off this project, and Brendan Duke, for being a constant sounding board. Resources used in preparing this research were provided to GWT and TD, in part, by NSERC, the Canada Foundation for Innovation, the Province of Ontario, the Government of Canada through CIFAR, Compute Canada, and companies sponsoring the Vector Institute: <http://www.vectorinstitute.ai/#partners>.

References

- [1] Samaneh Azadi, Catherine Olsson, Trevor Darrell, Ian J. Goodfellow, and Augustus Odena. Discriminator rejection sampling. *ArXiv*, abs/1810.06758, 2019.
- [2] Andrew Brock, Jeff Donahue, and Karen Simonyan. Large scale GAN training for high fidelity natural image synthesis. *ICLR*, 2018.
- [3] Joel Luis Carbonera and Mara Abel. A density-based approach for instance selection. In *2015 IEEE 27th International Conference on Tools with Artificial Intelligence (ICTAI)*, pages 768–774. IEEE, 2015.
- [4] Tong Che, Ruixiang Zhang, Jascha Sohl-Dickstein, Hugo Larochelle, Liam Paull, Yuan Cao, and Yoshua Bengio. Your gan is secretly an energy-based model and you should use discriminator driven latent sampling. *ArXiv*, abs/2003.06060, 2020.
- [5] Aidan Clark, Jeff Donahue, and Karen Simonyan. Efficient video generation on complex datasets. *arXiv preprint arXiv:1907.06571*, 2019.
- [6] Jia Deng, Wei Dong, Richard Socher, Li-Jia Li, Kai Li, and Li Fei-Fei. Imagenet: A large-scale hierarchical image database. In *2009 IEEE conference on computer vision and pattern recognition*, pages 248–255. Ieee, 2009.
- [7] Xin Ding, Z. Jane Wang, and William J. Welch. Subsampling generative adversarial networks: Density ratio estimation in feature space with softplus loss. *IEEE Transactions on Signal Processing*, 68: 1910–1922, 2020.
- [8] Kaiming He, Xiangyu Zhang, Shaoqing Ren, and Jian Sun. Deep residual learning for image recognition. In *Proceedings of the IEEE conference on computer vision and pattern recognition*, pages 770–778, 2016.
- [9] Martin Heusel, Hubert Ramsauer, Thomas Unterthiner, Bernhard Nessler, and Sepp Hochreiter. Gans trained by a two time-scale update rule converge to a local nash equilibrium. In *Advances in neural information processing systems*, pages 6626–6637, 2017.
- [10] Tero Karras, Samuli Laine, and Timo Aila. A style-based generator architecture for generative adversarial networks. In *Proceedings of the IEEE Conference on Computer Vision and Pattern Recognition*, pages 4401–4410, 2019.
- [11] Tero Karras, Samuli Laine, Miika Aittala, Janne Hellsten, Jaakko Lehtinen, and Timo Aila. Analyzing and improving the image quality of stylegan. *arXiv preprint arXiv:1912.04958*, 2019.
- [12] Tero Karras, Miika Aittala, Janne Hellsten, Samuli Laine, Jaakko Lehtinen, and Timo Aila. Training generative adversarial networks with limited data. *arXiv preprint arXiv:2006.06676*, 2020.
- [13] Tuomas Kynkänniemi, Tero Karras, Samuli Laine, Jaakko Lehtinen, and Timo Aila. Improved precision and recall metric for assessing generative models. In *Advances in Neural Information Processing Systems*, pages 3929–3938, 2019.
- [14] Dhruv Mahajan, Ross Girshick, Vignesh Ramanathan, Kaiming He, Manohar Paluri, Yixuan Li, Ashwin Bharambe, and Laurens van der Maaten. Exploring the limits of weakly supervised pretraining. In *Proceedings of the European Conference on Computer Vision (ECCV)*, pages 181–196, 2018.
- [15] Marco Marchesi. Megapixel size image creation using generative adversarial networks. *arXiv preprint arXiv:1706.00082*, 2017.
- [16] Leland McInnes, John Healy, and James Melville. Umap: Uniform manifold approximation and projection for dimension reduction. *arXiv preprint arXiv:1802.03426*, 2018.

- [17] Lars Mescheder, Andreas Geiger, and Sebastian Nowozin. Which training methods for gans do actually converge? *arXiv preprint arXiv:1801.04406*, 2018.
- [18] Muhammad Ferjad Naeem, Seong Joon Oh, Youngjung Uh, Yunjey Choi, and Jaejun Yoo. Reliable fidelity and diversity metrics for generative models. *arXiv preprint arXiv:2002.09797*, 2020.
- [19] Fajar Ulin Nuha et al. Training dataset reduction on generative adversarial network. *Procedia computer science*, 144:133–139, 2018.
- [20] J Arturo Olvera-López, J Ariel Carrasco-Ochoa, J Francisco Martínez-Trinidad, and Josef Kittler. A review of instance selection methods. *Artificial Intelligence Review*, 34(2):133–143, 2010.
- [21] F. Pedregosa, G. Varoquaux, A. Gramfort, V. Michel, B. Thirion, O. Grisel, M. Blondel, P. Prettenhofer, R. Weiss, V. Dubourg, J. Vanderplas, A. Passos, D. Cournapeau, M. Brucher, M. Perrot, and E. Duchesnay. Scikit-learn: Machine learning in Python. *Journal of Machine Learning Research*, 12: 2825–2830, 2011.
- [22] Tim Salimans, Ian Goodfellow, Wojciech Zaremba, Vicki Cheung, Alec Radford, and Xi Chen. Improved techniques for training gans. In *Advances in neural information processing systems*, pages 2234–2242, 2016.
- [23] Samarth Sinha, Anirudh Goyal, Colin Raffel, and Augustus Odena. Top-k training of gans: Improving generators by making critics less critical. *ArXiv*, abs/2002.06224, 2020.
- [24] Christian Szegedy, Vincent Vanhoucke, Sergey Ioffe, Jon Shlens, and Zbigniew Wojna. Rethinking the inception architecture for computer vision. In *Proceedings of the IEEE conference on computer vision and pattern recognition*, pages 2818–2826, 2016.
- [25] Michael E Tipping and Christopher M Bishop. Probabilistic principal component analysis. *Journal of the Royal Statistical Society: Series B (Statistical Methodology)*, 61(3):611–622, 1999.
- [26] Ryan C Turner, Jane Hung, Yunus Saatci, and Jason Yosinski. Metropolis-hastings generative adversarial networks. In *ICML*, 2018.
- [27] Xintao Wang, Ke Yu, Shixiang Wu, Jinjin Gu, Yihao Liu, Chao Dong, Yu Qiao, and Chen Change Loy. Esrgan: Enhanced super-resolution generative adversarial networks. In *Proceedings of the European Conference on Computer Vision (ECCV)*, 2018.
- [28] Yan Wu, Jeff Donahue, David Balduzzi, Karen Simonyan, and Timothy P. Lillicrap. Logan: Latent optimisation for generative adversarial networks. *ArXiv*, abs/1912.00953, 2019.
- [29] Saining Xie, Ross Girshick, Piotr Dollár, Zhuowen Tu, and Kaiming He. Aggregated residual transformations for deep neural networks. In *Proceedings of the IEEE conference on computer vision and pattern recognition*, pages 1492–1500, 2017.
- [30] Jiahui Yu, Zhe Lin, Jimei Yang, Xiaohui Shen, Xin Lu, and Thomas S Huang. Generative image inpainting with contextual attention. In *Proceedings of the IEEE conference on computer vision and pattern recognition*, pages 5505–5514, 2018.
- [31] Han Zhang, Ian Goodfellow, Dimitris Metaxas, and Augustus Odena. Self-attention generative adversarial networks. *arXiv preprint arXiv:1805.08318*, 2018.
- [32] Richard Zhang, Phillip Isola, Alexei A Efros, Eli Shechtman, and Oliver Wang. The unreasonable effectiveness of deep features as a perceptual metric. In *Proceedings of the IEEE Conference on Computer Vision and Pattern Recognition*, pages 586–595, 2018.
- [33] Shengyu Zhao, Zhijian Liu, Ji Lin, Jun-Yan Zhu, and Song Han. Differentiable augmentation for data-efficient gan training. *arXiv preprint arXiv:2006.10738*, 2020.
- [34] Yang Zhao, Chunyuan Li, Ping Yu, Jianfeng Gao, and Changyou Chen. Feature quantization improves gan training. *arXiv preprint arXiv:2004.02088*, 2020.
- [35] Bolei Zhou, Agata Lapedriza, Aditya Khosla, Aude Oliva, and Antonio Torralba. Places: A 10 million image database for scene recognition. *IEEE Transactions on Pattern Analysis and Machine Intelligence*, 2017.
- [36] Jiapeng Zhu, Yujun Shen, Deli Zhao, and Bolei Zhou. In-domain gan inversion for real image editing. *arXiv preprint arXiv:2004.00049*, 2020.

A Detailed Description of Evaluation Metrics

We use a variety of evaluation metrics to diagnose the effect that training with instance selection has on the learned distribution. In all cases where a reference distribution is required we use *the original training distribution*, and not the distribution produced after instance selection. Doing so would unfairly favour the evaluation of instance selection, since the reference distribution could be changed to one that is trivially easy to generate.

Inception Score (IS) [22] evaluates samples by extracting class probabilities from an ImageNet pretrained Inceptionv3 classifier and measuring the distribution of outputs over all samples. The Inception Score is maximized when a model produces highly recognizable outputs for each of the ImageNet classes. One of the major limitations of the Inception Score is its insensitivity to mode collapse within each class. A model that produces a single high quality image for each category can still achieve a good score.

Fréchet Inception Distance (FID) [9] measures the distance between a generated distribution and a reference distribution, as approximated by a Gaussian fit to samples projected into the feature space of a pretrained Inceptionv3 model. FID has been shown to correlate well with image quality, and is capable of detecting mode collapse and mode adding. However, FID does not differentiate between fidelity and diversity. As such, it is difficult to assess whether a model has achieved a good FID score based on good mode coverage, or because it produces high quality samples.

Precision and Recall (P&R) [13] were designed to address the limitations of FID by providing separate metrics to evaluate fidelity and diversity. To calculate P&R, image manifolds are created by first embedding each image in a given distribution into the feature space of a pretrained classifier. A radius is then extended from each data point to its K^{th} nearest neighbour to form a hypersphere, and the union of all hyperspheres represents the image manifold. Precision is described as the percentage of generated samples that fall within the manifold of real images. Recall is described as the percentage of real images which fall within the manifold of generated samples. A limitation of P&R is that they are susceptible to outliers, both in the reference and generated distributions. Outliers artificially inflate the size of the image manifolds increasing the rate at which samples fall into those manifolds. Thus, a model that generates diverse, but poor quality, samples can still achieve a good score.

Density and Coverage (D&C) [18] have recently been proposed as robust alternatives to Precision and Recall, which have been shown to be susceptible to outliers. Density can be seen as an extension of Precision which measures how many real image manifolds a generated sample falls within on average. Coverage is described as the percentage of real images that have a generated sample fall within their manifold.

B Insights for Applying Instance Selection to GANs

We found that, while instance selection could be used to achieve significant gains in model performance, some changes to other hyperparameters were necessary in order to ensure training stability. Here we detail some techniques that we found to work well in our experiments.

- **Reduce batch size** - Contrary to evidence from BigGAN [2] suggesting that larger batch sizes improve GAN performance, we found batch sizes larger than 256 to degrade performance when training with instance selection. We speculate that because we have simplified the training distribution by removing the difficult examples, the discriminator overfits the training set much faster. We posit that the smaller batch size could be acting as a form of regularization by reducing the accuracy of the gradients, thereby allowing the generator to train for longer before the discriminator overfits the training set and the model collapses.
- **Reduce model capacity** - Since the complexity of the training set is reduced when applying instance selection, we found it necessary to also reduce model capacity. Training models with too much capacity lead to early collapse, also likely caused by the discriminator quickly overfitting the training set.
- **Apply additional regularization** - We have not experimented much with applying GAN regularization methods to our models, but think that it could be important for combating the aforementioned discriminator overfitting problem. Applying techniques such as R1 regularization [17] or recently proposed GAN data augmentation [12, 33] could allow for

instance selection to be combined with the benefits of larger batch sizes and model capacity. We leave this investigation for future work.

C Retention Ratio Experiment Numerical Results

In Table 3 we include numerical results for the retention ratio experiments conducted in §4.4. These values accompany the plots in Figure 3. We also report the performance of BigGAN and FQ-BigGAN from [34] for comparison.

Table 3: Performance of models trained on 64×64 resolution ImageNet. A retention ratio of less than 100 indicates that instance selection is used. Best results in bold.

Model	Params (M)	Batch Size	Retention Ratio (%)	IS \uparrow	FID \downarrow	P \uparrow	R \uparrow	D \uparrow	C \uparrow
BigGAN [2]	52.54	512	100	25.43	10.55	-	-	-	-
FQ-BigGAN [34]	52.54	512	100	25.96	9.67	-	-	-	-
SAGAN [31]	23.64	128	100	17.77	17.23	0.68	0.66	0.72	0.71
			90	18.98	15.85	0.70	0.66	0.75	0.74
			80	21.62	13.17	0.74	0.65	0.87	0.79
			70	23.95	11.98	0.75	0.64	0.92	0.82
			60	27.95	10.35	0.78	0.63	0.99	0.87
			50	31.04	9.63	0.79	0.62	1.07	0.88
			40	37.10	9.07	0.81	0.60	1.12	0.90
			30	41.85	9.75	0.83	0.55	1.19	0.90
			20	43.30	12.36	0.82	0.49	1.17	0.88
			10	37.16	19.24	0.79	0.33	1.07	0.78

D Sample Sheets

We generate several different sample visualizations in order to better understand the impact that instance selection has on GAN behaviour. All samples in this section are from BigGAN models trained on 128×128 resolution ImageNet.

To evaluate whether models trained with instance selection learn a semantically meaningful representation, we interpolate between classes in Figure 8. We observe smooth transitions between classes, which indicates that the GAN has learned a useful representation and not simply memorized the training set.

The impact of instance selection on sample fidelity is evaluated by comparing samples from randomly selected classes for both a baseline model trained on the full dataset (Figure 9a) and a model trained with instance selection (Figure 9b). Sample fidelity is judged based on whether an ImageNet pretrained Inceptionv3 classifier can successfully identify the contents of each image. We observe that the classifier correctly recognizes a larger percentage of the samples from the GAN trained with instance selection, indicating that they are more consistent with their class on average than the baseline model.

In Figures 10 and 11 we compare the result of applying the truncation trick to a baseline model and a model trained with instance selection in terms of visual sample quality. The baseline model initially produces some unrealistic samples which do not resemble the target class (e.g. columns 3, 5, and 9). The quality of these samples improves as the truncation threshold is lowered. The model trained with instance selection does not initially produce any samples with egregious errors, but it still benefits from the truncation trick, such as improvements to details in the wolves’ faces.

To better understand how instance selection affects sample diversity, we visualize image manifolds of different datasets and models by organizing images in 2D using UMAP [16] (Figure 12). We only plot a single class so that we can see variations across the image manifold in greater detail than if multiple classes were plotted simultaneously. All image samples share the same 2D embedding, such that manifolds are comparable between datasets and models. We observe that even though

instance selection has removed 50% of the images from the original dataset (Figure 12a), it still retains coverage over most of the original image manifold (Figure 12b). Only images containing extreme viewpoints are omitted. The GANs trained on the original and reduced datasets both cover less of the image manifold than their respective source datasets. While the baseline GAN (Figure 12c) covers more of the image manifold than the GAN trained with instance selection (Figure 12d), samples from these extra regions often appear less realistic.

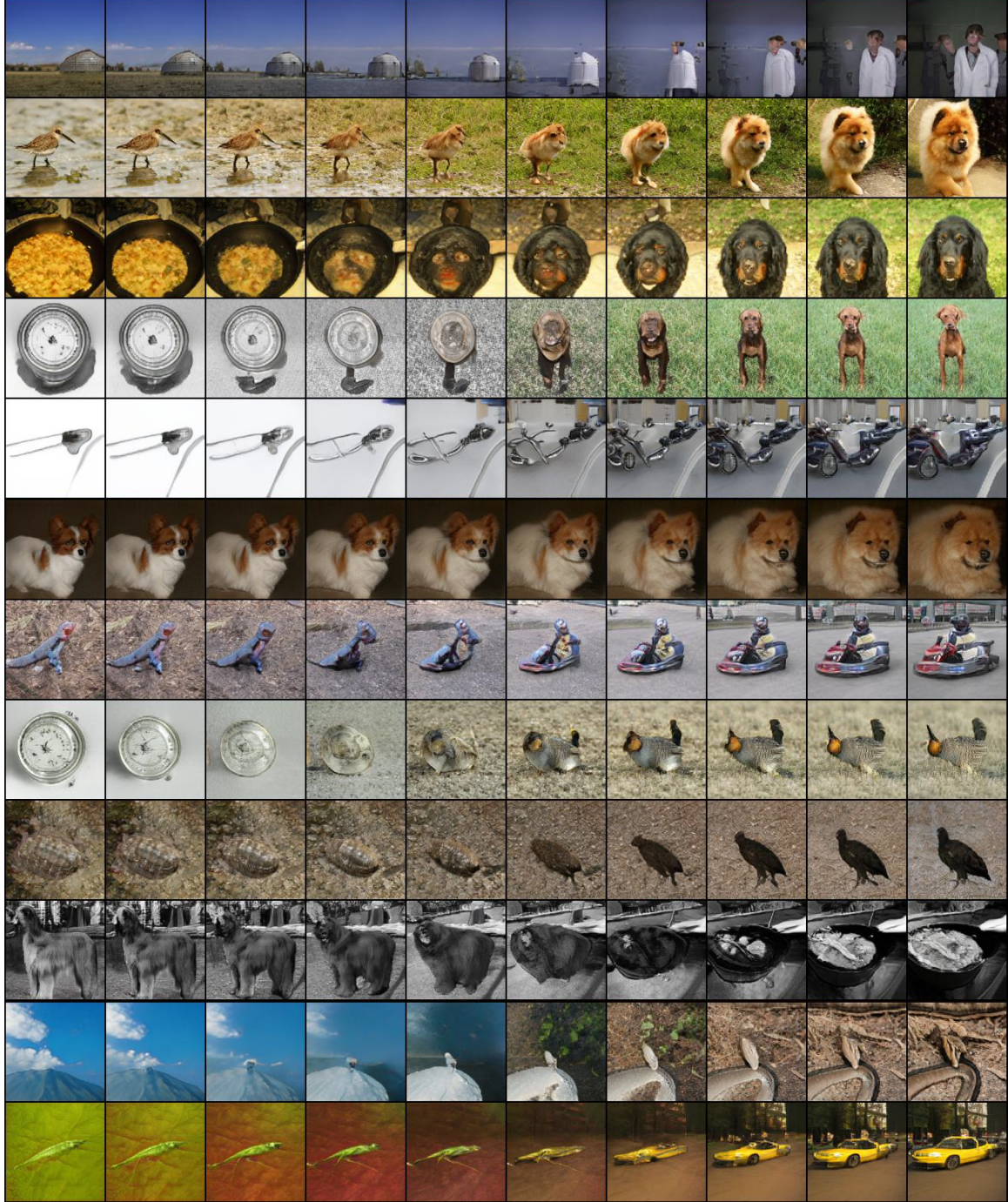


Figure 8: Interpolation between classes from 128×128 BigGAN trained with instance selection (50% of ImageNet dataset). Samples interpolate between classes smoothly, indicating that the model has learned a semantically meaningful representation, and has not simply memorized the training set.



(a) Baseline (100% of dataset)



(b) w\ Instance selection (50% of dataset)

Figure 9: Uncurated samples from BigGAN models trained on 128×128 resolution ImageNet. Each row is conditioned on a different randomly selected class. Red borders indicate misclassification by a pretrained Inceptionv3 classifier. The model trained with instance selection is much more likely to produce samples that resemble the target class.

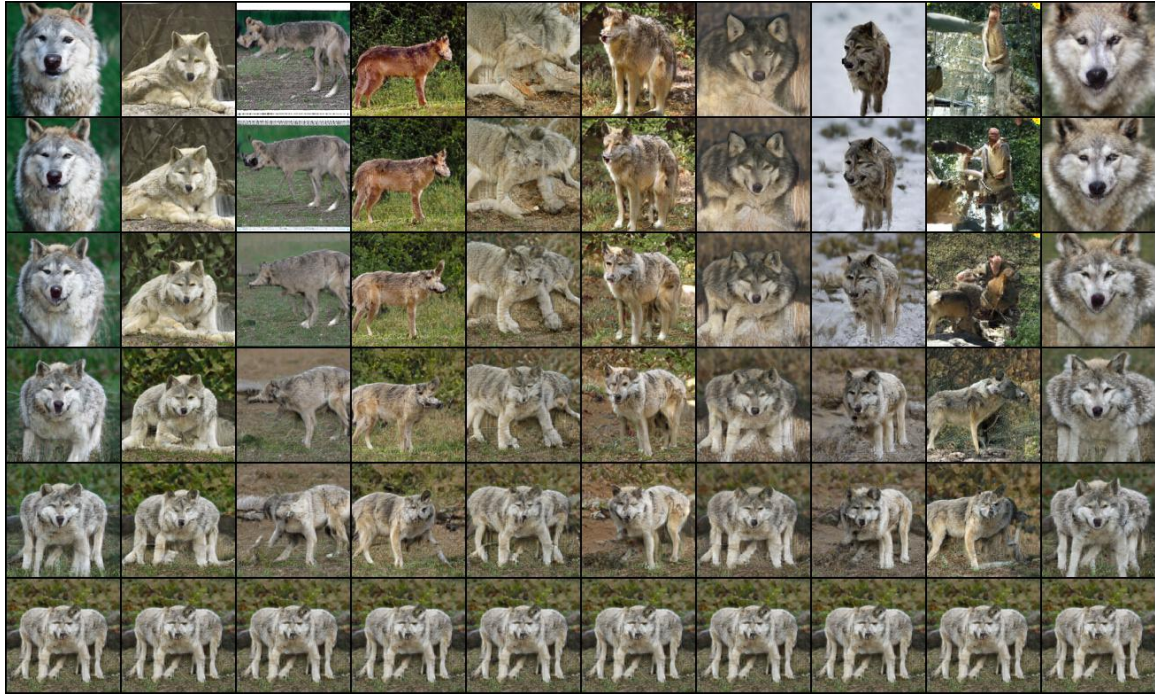
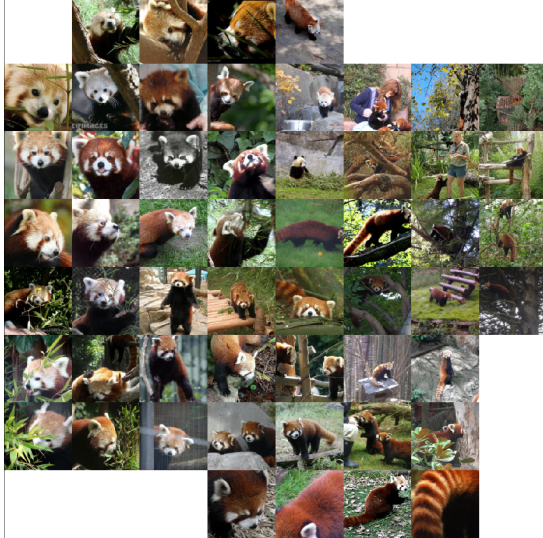


Figure 10: Samples for the grey wolf class from the baseline model trained on the full dataset. Each column shares the same latent vector, and each row shares the same truncation threshold. Truncation threshold ranges from 1 (top row) to 0 (bottom row). Significant truncation is required before all samples resemble the target class.



Figure 11: Samples for the grey wolf class from model trained with instance selection (50% of dataset). Each column shares the same latent vector, and each row shares the same truncation threshold. Truncation threshold ranges from 1 (top row) to 0 (bottom row). Most samples resemble the target class without any truncation.



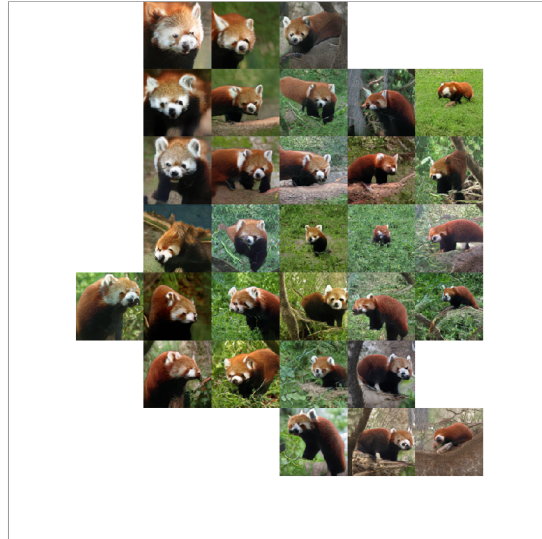
(a) Full dataset



(b) Dataset after 50% instance selection



(c) Samples from GAN trained on full dataset



(d) Samples from GAN trained on 50% of dataset

Figure 12: Visualization of the image manifolds for the red pandas class from (a) the full ImageNet dataset, (b) the dataset after 50% instance selection, (c) samples from a GAN trained on the full dataset, and (d) samples from a GAN trained on 50% of the dataset. Manifolds are created by embedding all images into an Inceptionv3 feature space, then projecting them into 2D with UMAP [16]. All images share the same 2D embedding such that subplots are comparable. Instance selection removes images from the dataset that have unusual viewpoints or pose. Both GANs appear to cover less of the image manifold than their respective source datasets. The GAN trained on the full dataset covers some regions of the image manifold that are not covered by the model trained with instance selection, however, these regions are more likely to appear unrealistic.